Bulk Heterojunction Organic Photovoltaics

Samuel James Bader
MIT 3.15: Electrical, Optical, and Magnetic Materials and Devices
(Dated: May 6, 2013)

This paper discusses the device physics, architecture, and engineering challenges of bulk heterojunction organic photovoltaics (BHJ OPVs), one of the most promising technologies for the economic, large-scale, and sustainable generation of solar power. The focus is on explaining the variety of materials choices, recent advances, and continuing research spanning a wide range of sciences and disciplines toward the goal of mass-producible organic solar cells.

I. INTRODUCTION

As the need for renewable and non-polluting energy sources spurs the progress of research, organic photovoltaics have become an increasingly promising technology for harvesting solar power in an economically practical manner.

While organic photovoltaics, OPVs, are generally not as efficient as the silicon-based solar cells which currently dominate the solar market, their advantage lies in the promise of low-cost, high-throughput, non-vacuum-based manufacturing (such as ink printing and roll-to-roll processing), the use of inherently cheap and non-toxic organic materials, and their potential for flexible, lightweight cells. Given these improvements, the economics of solar power may prefer a slightly less efficient but cheaper and safer technology [7].

Additionally, the versatility of the materials involved create a fundamentally interesting materials engineering problem involving a broad range of physical, chemical, and nano-engineering concerns. This paper will address the physics and creative architecture of the most promising of these devices, the bulk heterojunction organic photovoltaic (BHJ OPV), and the relevent materials choices, processing techniques, and recent advances bringing this science ever closer to the market.

Section II introduces the basic device physics necessary to understand the operation of an organic solar cell, beginning by analogy with conventional inorganics. Section III then applies that understanding to explain the ideal architecture for an organic cell: the bulk heterojunction. Section IV then uses the constraints of that architecture (mainly related to the band structure) to explain the present choices of materials for the active layer (the donors and acceptors). Section V then describes the processing techniques necessary for high-throughput production of OPVs, and the constraints of that process are used to inform the choice of materials for the auxilary layers (charge transport layers and electrodes). Section VI then discusses recent proposals to improve the current OPV materials choices, mainly by the addition of new carbon materials, and Section VII summarizes the discussion and provides an outlook on the future of OPVs.

II. PRINCIPLES AND DEVICE PHYSICS

II.1. Analogy: inorganic solar cells

Much of the terminology and operation of organic solar cells is imported from their silicon predecessors, and throughout this discussion, a familiarity with the principles of conventional, inorganic photovoltaics will generally be assumed. For reference, the following briefly summarizes conventional photovoltaics with a focus on the aspects that differ in discussion of organic devices.

The standard silicon photovoltaic is a bilayer device, a classic *p*-*n* junction. Absorbed light creates free electron-hole pairs, which are effectively uncoupled from one another due to the strength of dielectric screening. The generated minority carriers which diffuse into the strong electric fields of the depletion region form a drift photocurrent which is collected at the electrodes. When operated in the proper I-V regime, this current can supply power to a load.

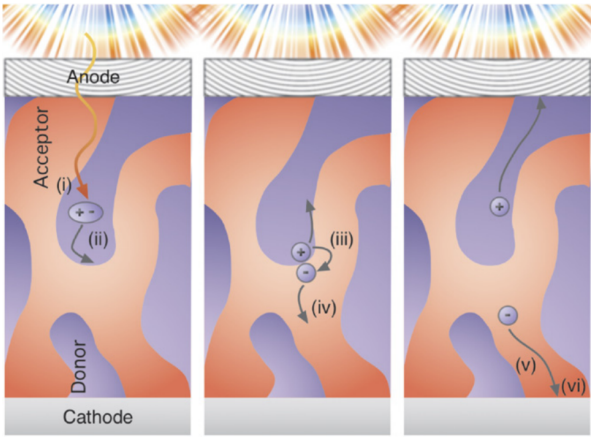

FIG. 1: The six stages of organic photocurrent generation: exciton generation, exciton diffusion, dissociation, charge transport, and extraction. The reason for the strange, curved appearance of the Donor-Acceptor interface will be clarified shortly. Reprinted from [6].

In contrast, the stages of a organic photocurrent generation [6] are depicted in Figure 1. First, (i) absorbed light

generates an exciton (bound electron-hole pair), which then (ii) diffuses to a "donor-acceptor" interface. At the interface, the exciton (iii) dissociates into free carriers, which (iv) travel via hopping transport to be (vi) extracted at the electrodes.

The journey is clearly more complicated, and the physical details of the above-mentioned processes constrain the material and architectural choices, so they are discussed in in combination with the device architecture after the general principles of organic conduction are explained below.

II.2. Energies and excitations

Whereas charge transport in inorganic semiconductor materials stems from the nearly free carriers in a crystalline band structure, conduction in disordered organic materials is better described by hopping between bound, localized states [6].

When a carbon atom, with its ground state $1s^2 2s^2 2p^2$, bonds to two or three other atoms, the σ bonds are sp^2 hybridized, which leaves one electron per carbon atom in a p_z orbital. The level of p_z orbitals is split into two delocalized bands of molecular orbitals: bonding (π) and antibonding (π^*). These levels are also known respectively as the Highest Occupied Molecular Orbital (HOMO) and Lowest Unoccupied Molecular Orbital (LUMO). With typical energy separations of one to three electron volts, the HOMO and LUMO are analogous, in role, to the valence and conduction bands of inorganic semiconductors.

However, because the carrier transport proceeds by tightly-bound hopping, mobilities in organics are much lower than in semiconductors. As discussed in [5], many factors affect charge mobility in organics, including molecular packing, disorder, temperature, elecric field, impurities, pressure, carrier density, and size/molecular weight, the end result being that mobilities in the materials used for organic semiconductors[1] are on typically on the order of ∼1 cm/Vs, as compared with several hundred or a thousand cm/Vs in silicon [8].

Furthermore, in organic semiconductors, free electrons and holes are not the only important excitations. Because organic materials, with dielectric constants ε of about 3 or 4, do not screen charge as effectively as silicon, excited electrons and holes will prefer to remain together as *exciton* pairs. These quasiparticle states have binding energies on the order of .5-1eV [18], far above the available thermal energy (25meV). [2] Since excitons have no net charge, they cannot conduct a current unless they are dissociated first. Solving this problem will be the main focus of Section III.

[1] Other than in lower-dimensional special cases like graphene, carbon nanotubes, etc, which will come up further on.

[2] In comparison, exciton binding energies in silicon are on the order of 10-20meV [4, 9], so silicon excitons are thermally dissociated, and generally disregarded.

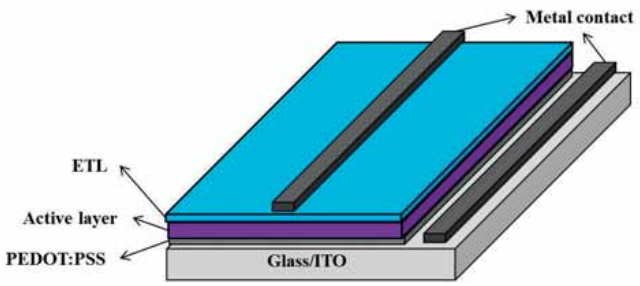

FIG. 2: Typical single-junction organic solar cell architecture. One of the two contacts is glass/ITO so that sunlight can illuminate the junction. The exciton creation, diffusion, dissociation, and charge transport occur in the active layer, and the other layers ensure one-way charge transport. Note that an inverted structure of this type is also in common use. Reprinted from [18].

III. ARCHITECTURE

To the extent discussed thus far, the device geometry may be visualized as in Figure 2, which will become more clear as the individual layers and choices are explained below.

III.1. Active layer: the bulk heterojunction

The first organic solar cells [6] were simpler than Figure 2: essentially a single-material active layer, encased by two electrodes with different workfunctions. Light created excitons in the active layer, wherein they ideally diffused to the contacts to dissociate and provide a current. These devices relied on thermal effects and the contact interface for exciton dissociation

However, as the exciton energy scaling (See Sec. II.2) demonstrates, thermal dissociation is ineffective, and, as mentioned in [6], dissociation at the contacts does not contribute strongly either. Additionally, the active layer was generally much thicker than the exciton diffusion length, so most excitons simply recombined and re-radiated their energy. As a result, these devices suffered power-conversion efficiences far below 1%.

The introduction of a second material is necessary to provide an interface where the fields are sufficient to dissociate an exciton [18]. Upon dissociation, the material which keeps the hole is refered to as the "donor," and the one which receives the electron is referred to as the "acceptor," whereas the entire structure is often called the Donor-Acceptor (D-A) interface.[3] The first such "bi-

[3] It is worth emphasizing a subtlety of the names here. The "donor" material, because it receives a photogenerated hole, is occasionally refered to as the "*p*-type material" in analogy with

layer" solar cells were demonstrated by Tang in the 1980s [6].

The concept behind a D-A interface is depicted in the HOMO-LUMO band structure of Figure 3. If the acceptor LUMO is below the donor LUMO by an amount greater than the exciton binding energy, the system can lower its energy by dissociating the exciton pair across the interface. The constraints which this places on the band structure engineering of the donor (typically a conjugated-chain polymer) and acceptor (typically a fullerene derivative) will become important in the discussion of material choices.

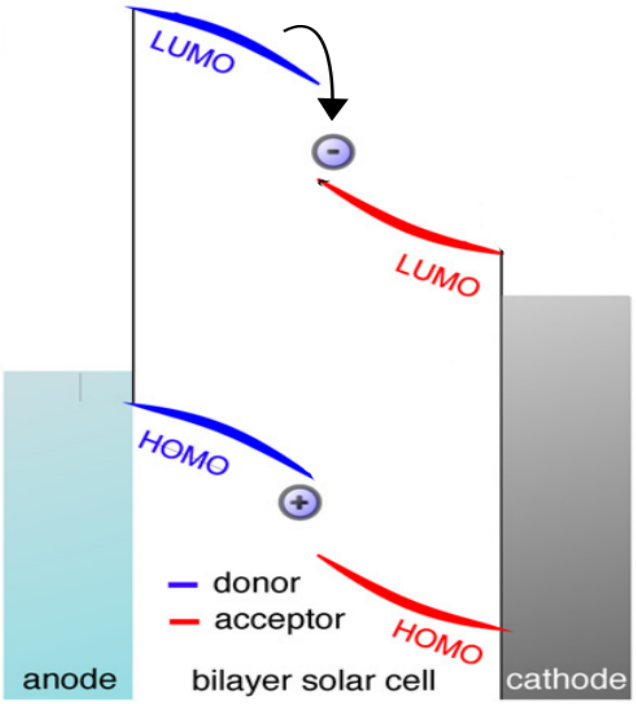

FIG. 3: A generic D-A interface: if the LUMO of the acceptor is sufficiently below that of the donor, the exciton may lower its energy by dissociating. Modified from [6].

However, this simple bilayer structure leads to an impossible trade-off [6]. The absorption length scales for these organic materials (hundreds of nm) are many times greater than the exciton diffusion length scale ($\sim$ 10nm), so if the material is thick enough to absorb a significant amount of solar power, it is necessarily so thick that most of that power is lost to radiative recombination of the excitons.

In the 1990s, a new solution emerged: "bulk heterojunction" active layers, which mix the donor and acceptor materials together [19]. Though the fullerene and conjugated polymers are blended, each type will tend to form aggregate domains which then serve a dual purpose of (1) distributing the D-A interface throughout the entire bulk of the active layer and (2) providing "percolation pathways" (contiguous chains of each domain) for charge transport through each layer after dissociation. As such, the ideal morphology of the active layer is an "interpenetrating D-A network" where the dimensions of each small domain are below the exciton diffusion length [18]. In this manner, every point of the layer can be within a diffusion length of a D-A interface, justifying the name *bulk* heterojunction [19].

In a bulk heterojunction (BHJ), the thickness trade-off now becomes that the active layer must be deep enough to absorb light, but not so deep that separated carriers recombine along their routes to the contacts (since the distributed D-A interface will support recombination just as it supports dissociation). Generally, an active-layer thickness of 100-150nm satisfies both criteria, and state-of-the-art devices featuring this architecture have increased their power conversion efficiency from 2.5% up toward 11% over the past decade [18].

III.2. Auxilary layers

As in Figure 2, the substrate in these devices is often a transparent (to pass the sunlight) conductive layer, such as glass/ITO, whose work function is near the donor HOMO to support hole extraction. The other metal contact should have a lower work function near to the LUMO of the acceptor to support electron extraction.

Generally, an Electron Transport Layer (ETL) and a Hole Transport Layer (HTL) are included to "match" the electrode work functions to the HOMO/LUMO bands and provide better one-way charge transport/injection. In Figure 2, as is often the case, the HTL is a layer of PEDOT:PSS, for reasons which will be discussed in Sec. V.

Given the constraints of this architecture, we may now begin to discuss the materials necessary to achieve it.

IV. MATERIAL CHOICES

IV.1. Bandgap considerations

Many of the important decisions regarding the donor and acceptor selections are determined by the requirements of the cell's band structure. The important quantities to balance are marked in Figure 4.

The energies to note are as follows:

E_g: Since the donor is typically the main absorber, the absorption cut-off at the donor HOMO-LUMO bandgap selects what portion of the solar spectrum will be available to the cell. The peak wavelength of the solar spec-

a convential photovoltaic (for example, [2]). It is an unfortunate confusion of names that the *p*-type material in convential photovoltaics is doped with "acceptor" atoms.

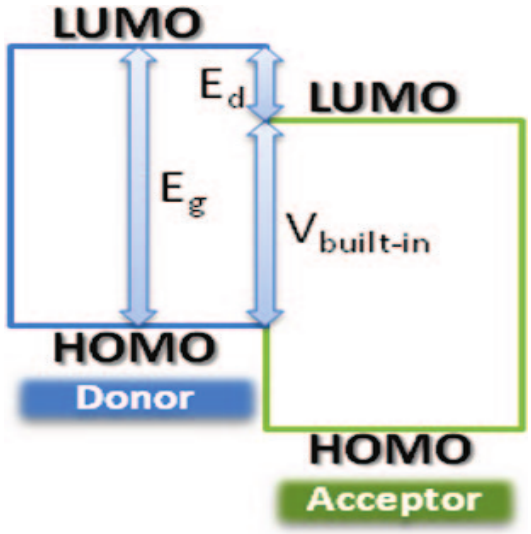

FIG. 4: The important energy differences in the D-A interface are E_g, the bandgap in the donor, E_d, the difference in the LUMO levels, and V_{OC}, the open-circuit/built-in voltage. Reprinted from [2].

trum is at 700nm (1.77eV), which is a relatively small gap for a typical donor material [2].

E_d: In order for an exciton in the donor to preferentially dissociate, the acceptor LUMO must present an energy drop competitive with the exciton binding energy. As noted in [2], about ∼.3eV is a reasonable minimum value to favor the electron transfer from a conjugated polymer donor to a fullerene derivative acceptor.

V_{OC}: After dissociation, the electron is in the acceptor LUMO and the hole is in the donor HOMO, so the gap between those two levels sets a maximum on the energy available for any attached load. In fact, the other band-banding and any offsets from the contact work functions can be shown to cancel, such that the open-circuit voltage is nearly just given by this energy difference [3].

So the important trade-off from basic bandgap considerations is the simultaneous demand to maintain a low E_g for better absorption, but a sufficiently high V_{OC} or E_d. As can be seen in Figure 4, these constraints work against one another; this difficulty will inform the selection of an acceptor and heavily constrain the choice of donor.

IV.2. Acceptor

Fullerene derivates are the standard acceptor material in organic photovoltaics. Several distinct advantages mark Buckminster-fullerene (C_{60}) as an ideal base molecule for this purpose [2]. First, its low LUMO level gives it a thermodynamic disposition to accept electrons from a donor material. In fact, the C_{60} LUMO is triply degenerate, such that, with its unique ability to stabilize negative charges, a single C_{60} can accept up to six electrons at a time. Finally, the the timescale for a photo-induced electron transfer from a conjugated polymer donor to C_{60} is 45fs, many orders of magnitude faster than exciton decay or the reverse electron transfer. In addition to improving the quantum efficiency of charge separation to near unity, this ability to rapidly quench the excitons from a highly reactive excited donor improves the photostability of the devices by reducing the chance that the donor will photooxidize (eg with oxygen from the environment).

However, certain modifications [2] are necessary in order to make C_{60} compatible with the solution-based fabrication process (processing will be discussed more further on). As is, C_{60} shows poor solubility, and actually tends to crystalize. Wudl and Hummelen solved this problem in 1995 by functionalizing the fullerene with solubilizing groups to produce [6,6]-phenyl-C_{61}-butyric acid methyl ester (PCBM), shown in Figure 5. PCBM still suffers one drawback in that its structural symmetry disallows low-energy transition, reducing its visible absorption; however, this can also be remedied by upgrading to the use of a higher fullerene, C_{70}, to generate $PC_{71}BM$, whose reduced symmetry increases visible absorption (also shown in Figure 5).

Further additives may be used to decrease the size of the potentially troublesome $PC_{71}BM$ grain boundaries (so that domain dimensions stay short). Other fullerene derivatives (with higher LUMOs to increase V_{OC}) which have received significant attention include bis-$PC_{61}BM$, tris-$PC_{61}BM$, and indene-fullerene bisadduct ICBA [18].

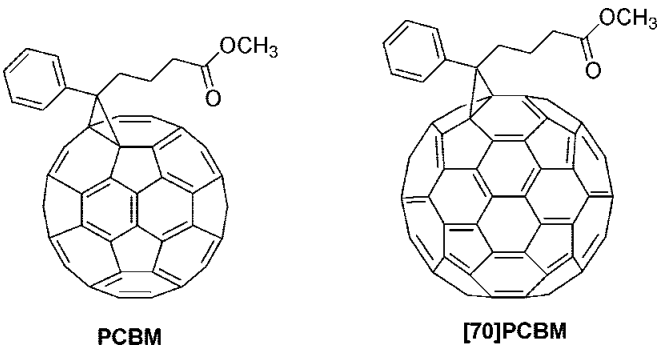

FIG. 5: Chemical structures for $PC_{61}BM$ and $PC_{71}BM$, the latter of which shows improved visible absorption, along with the many advantages of the former. The attached functional group improves the solubility of both fullerene molecules, essential for solution processing.

IV.3. Donor

At this point, fullerenes fulfill the need for an acceptor layer, and future improvements to organic solar cells are far more likely to target the donor [2], which has to satisfy several material constraints [18].

Of course, good electrical properties (mobility) and solubility are important, as with the acceptor. But band structure constraints add another layer of difficulty; these constraints are essentially those mentioned at the beginning of this section, but with the acceptor properties held fixed (since the acceptor is known). (1) A smaller HOMO-LUMO gap is desired to broaden absorption within the solar spectrum, (2) the HOMO should be low to increase V_{OC}, and (3) the LUMO should be sufficiently higher than that of the fullerene.

The most promising materials for this purpose are *conjugated polymers*, which have already impacted advances in organic conductors, OFETs, and OLEDs [2]. These are polymer chains with alternating single and double bonds along the backbone. The main advantage to conjugated polymers is the extent to which the they can be engineered by changing the repeating backbone unit, the side chains, and the substituents [18]. Several of these approaches to "bandgap engineering," depicted in Figure 6, will be discussed at a conceptual level, following the more detailed coverage in [2].

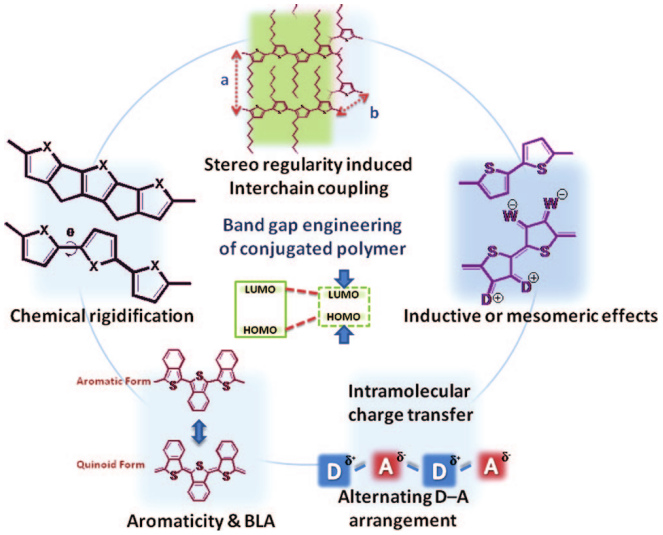

FIG. 6: Several promising approachings for engineering the HOMO-LUMO gap in conjugated polymers. Reprinted from [2].

IV.3.1. Aromaticity

The first approach in the band engineering of the conjugated polymers concerns the aromaticity–that is, ability to adopt and stabilize excess charge–of its repeating backbone units. As shown in Figure 7, a typical polyaromatic chain will have two resonant structures: an "aromatic form," where the electrons concentrate in double bonds of the aromatic structures, and a "quinoid form," where the electrons concentrate into double-bonds linking those units.

Since the quinoid form as a ground state does not take

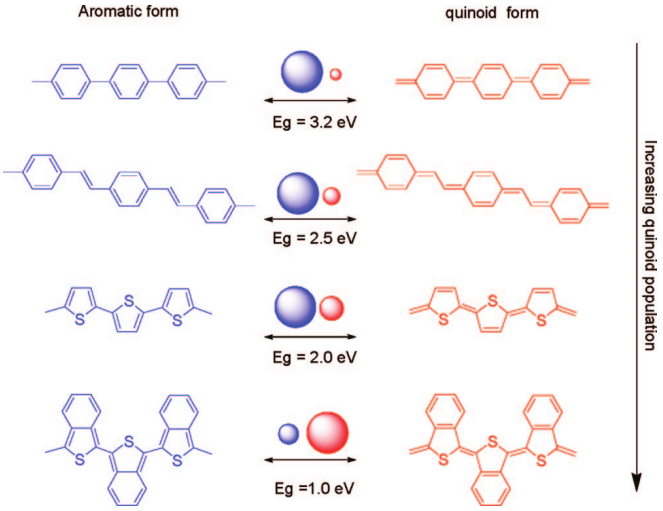

FIG. 7: Aromatic and Quinoid forms of several polymers. The relative population of bonds in each form for a specific polymer is indicated by the size of the colored circles, and one sees that increasingly quinoid polymers result in lower bandgaps. Reprinted from [2].

advantage of the aromaticity of the repeating units in stabilizing delocalized electrons, quinoid forms lead to higher HOMO levels, reducing the bandgap [2]. Figure 7 shows four examples:

1. The topmost polymer is polyphenylene, simply a chain of benzene molecules, wherein the aromatic form dominates and the bandgap is resultingly high, 3.2eV.

2. Diluting the benzenes' aromaticity via double-bonds on the links leads to the second polymer shown: poly(phenylenevinylene), where the band gap is reduced to 2.5eV.

3. Or, by substituting a sulfur for one of the carbons, one obtains thiophene, which is less aromatic than benzene, bringing the bandgap down to 2.0eV.

4. One final creative method is to use the thiophene chain, but attach a more aromatic benzene to each (polyisothianaphthene). Since the quinoid form of the chain can take advantage of the aromaticity of the benzenes at the expense of the thiophenes, the quinoid form actually dominates, lowering the bandgap to 1.0eV.

Quinoidization approaches have also demonstrated success with several other polymers, eg poly(thieno[3,4-b]pyrazine) and poly(thieno[3,4-b]-thiophene). In fact, the most common donor material is poly(3-hexylthiophene), known as P3HT.

IV.3.2. Chemical rigidification

Since the conjugation and delocalization of electrons relies on an overlap between neighbooring π-bonds (p_z), only coplanar units of the chain can show significant conjugation. Attaching groups which hinder rotation between neighbooring units can planarize the polymer (that is, align the aromatic units so that all the π_z bonds are parallel), and thus increase the effective conjugation length for the electrons.

Beginning from the third polymer in Figure 7, one finds that multiple possible modifications, shown in Figure 8, can sterically prevent rotation about the links. Other factors, such as sidechain coupling (as indicated in Figure 6) also support planarization.

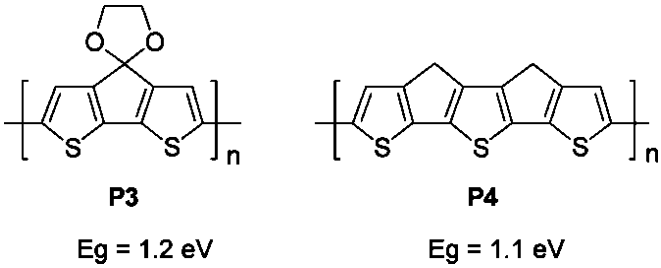

FIG. 8: Attaching groups to rigidify the thiophene chain against rotation. Reprinted from [2].

IV.3.3. Substituents

Incorporation of various substituent atoms or groups may also be used to perturb the energy structure via inductive effects (that is, having to do with the relative electronegativities) or mesomeric effects (that is, affecting the resonant structures). Regardless of which effect is involved, substituents which tend to donate electrons will generally raise the HOMO, and substituents which tend to withdraw electrons will generally lower the LUMO. This is demonstrated in Figure 9 with the addition of an electron-donating alkoxy group (P5) and the addition of both amino (electron-donating) and nitro (electron-withdrawing) groups (P6).

IV.3.4. Push-pull conjugation

The most successful strategy [18] has been the incorporation of electron-donating (push) and electron-accepting (pull) groups directly into the chain to form *push-pull conjugated polymers*. The idea is depicted in Figure 10. The push group has, by definition, a higher HOMO and, generically, a higher LUMO that the pull group. When these two types are combined in an alternating chain, the HOMO and LUMO orbitals mix to form molecular orbitals in which the energies of each level split, following

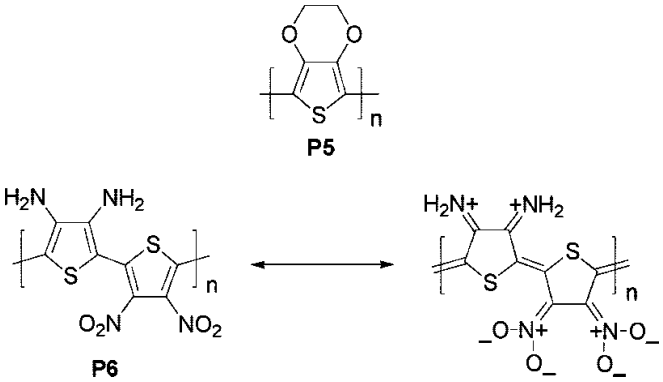

FIG. 9: The addition of an electron-donating group (P5) lowers the polythiophene bandgap to 1.5eV (from 2eV in Figure 7). Adding both donating and withdrawing groups (P6) can lower it further to 1.1eV. Reprinted from [2].

basic perturbation theory. This splitting forces the polymer HOMO closer to the polymer LUMO. Two concrete examples [2] are given in Figure 11 to demonstrate the range of bandgap engineering available by careful choice of push and pull substituents.

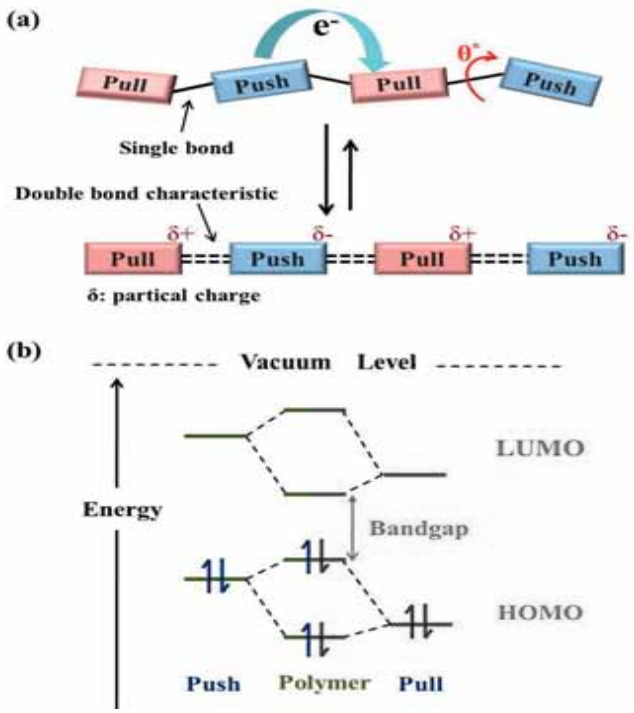

FIG. 10: An intuitive perturbation diagram showing how push-pull architecture shrinks the bandgap. Reprinted from [18].

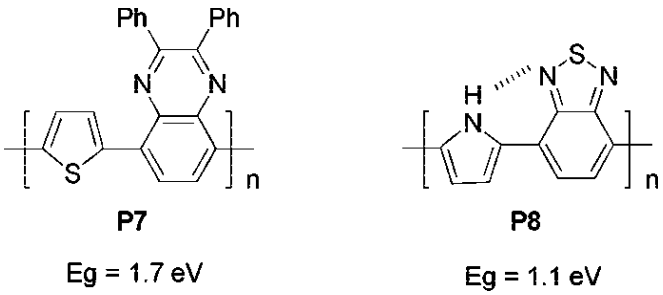

FIG. 11: Examples of push-pull conjugated polymers. The reduction in band gap depends on the strength of the push and pull features. The donor and acceptor are both relatively weak in P7 (thiophene and quinoxaline), and strong in P8 (pyrrole and benzodiathiazole). Reprinted from [2].

IV.3.5. Other desirable properties

It is also worth mention that the various techniques for bandgap engineering in this section also affect the electrical characteristics of the material. Fortunately, strong delocalization of the electron orbitals and ordered, planar channels contribute positively to the charge transport properties of the conjugated polymers.

Finally, one other major objective in the material engineering is that the polymer be soluble for processing purposes; however, strong $\pi - \pi$ stacking interactions between chains often render promising conjugated polymers insoluble. This effect can be countered via the addition of aliphatic side-chains, particularly branched alkyl groups to interfere with the stacking. The trade-off is that the addition of these insulating groups does diminish the charge-transport properties of the material, and this must be taken into account.

V. MANUFACTURE

V.1. Roll-to-Roll Processing

One major advantage to organic photovoltaics is the promise of cheaply printing off large-area solar cells en masse along giant ribbons of flexible substrate. Up until this point, the discussion has largely ignored this promise, reporting on successful material architectures for OPVs without concern for how to actually produce them. Krebs et al [15] open with a harsh criticism of this practice:

> "...there are challenges that have perhaps been taken too lightly in laboratory reports. Often tiny spin coated devices prepared on rigid glass through toxic solvent processing and metal evaporation is said to be roll-to-roll and industry compatible. The view held here is that claiming to be roll-to-roll and industrially compatible without such instruments is similar to claiming that one can learn how to swim on a floor..."

Whereas current test devices in experiments are often produced, as mentioned, via spin-coating, with toxic components, on inflexible materials, and using other such techniques unsuitable for mass production, the goal is to take advantage of the streamlined manufacturing ability suggested by flexible, solution-processed organics, rather than expensive fabrication procedures for silicon devices. One would hope that OPVs could just be processed "roll-to-roll" as in Figure 12 or Figure 13, and laminated at the end to protect the cell.

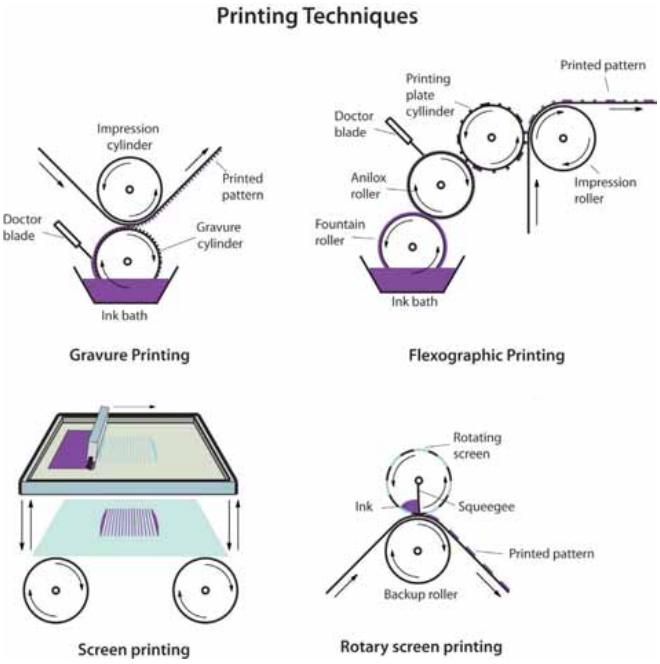

FIG. 12: Visualization of various contact printing techniques in common use and applicable to organic photovoltaic testing or mass production. Other techniques include coating (such as in Figure 13) or inkjet-type printing. Reprinted from [15].

V.2. Inks

One of the most important obstacles to mass production is the current dependence on toxic or polluting solvents in the inks of these device layers. Ideally, all layers would be printed from a solution based on water (or perhaps certain alcohols); at current, PEDOT:PSS (the hole transport layer in Figure 2) is just about the only component which satisfies this demand [15].

Three categories of ink are shown in Figure 14: dissolved material (wherein each particle is separately in solution), emulsions (where additives form micelle structures to keep the material in solution), and particulates

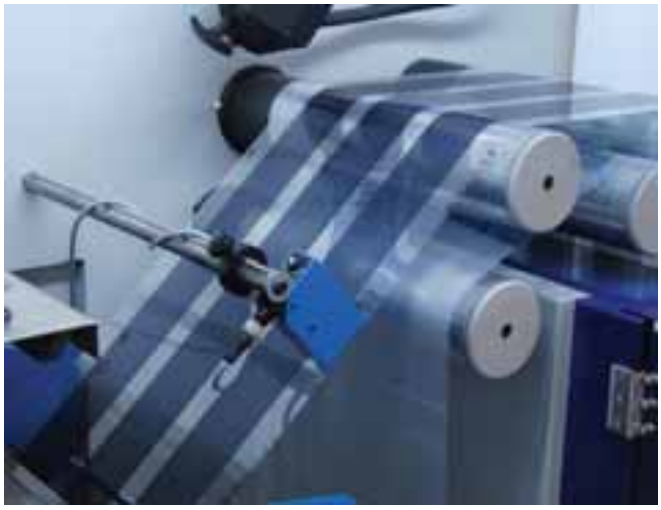

FIG. 13: Another possible means of roll-to-roll processing, "slot-die" coating, showing (in total) 48 stripes of an OPV active layer coated simultaneously. Reprinted from [15].

or pastes (where the material is suspened as solid particles). Since each type allows for the inking of different materials, careful planning may allow multiple ink formulations to replace the current technique of orthogonal solvents (that is, alternating polar and non-polar for each layer) [15].

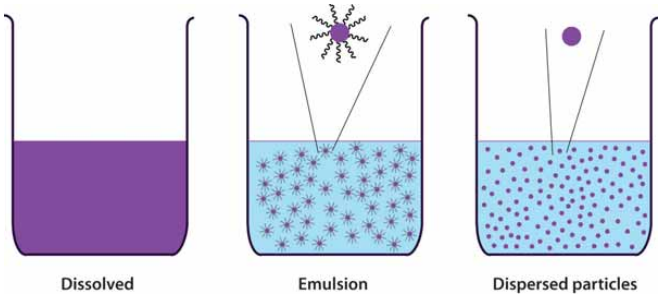

FIG. 14: Depiction of the three major categories of inks. Reprinted from [15].

V.3. Prospects for each layer

Whereas the device physics directly restricted the material choices for the active layer as discussed in Sec IV, the above manufacturing demands place the main constraints on the charge transport and electrode materials.

Silver is currently the main candidate for the non-transparent electrode. Silver pastes (high-viscosity with large particles or low-viscosity with nanoscale particles) are commercially available, though sintering may be necessary to acheive good conductivity with smaller particle sizes [15]. Furthermore, it is simple to make aqueous silver inks by combining silver flakes, aqueous binders, and water under heating; this procedure has been successfully demonstrated in solar cell fabrication [14].

As for the transparent electrode, ITO is the standard choice, although perhaps not for long; Sec. VI will discuss in great depth recent efforts to replace ITO with cheaper alternatives.

For the hole transport layer, PEDOT:PSS is a universal choice. This particular polymer can be simply processed from aqueous solution [15], and has an appropriate band structure to facilitate hole injection into a typical acceptor. It also serves two other purposes simultaneously [16]: (1) to planarize the rough ITO surface (which prevents accidental shunting through the thin-film layers), and (2) to provide a more chemically compatible effective substrate for the organic layers above (ie prevent dewetting of the other layers).

And finally, for the electron transport layer, the only material which seems to have been successfully used in a manner compatible with solution-processing is zinc oxide, which can be printed from water, methanol, or acetone [14, 15].

There is still much progress to be made in terms of efficient cells made entirely by sustainable, high-throughput means, though acceptable processes have been used for currently less-efficient cells [14].

VI. THE "ALL-CARBON" ADVANCES

Most recently, proposed improvements to the above structures have typically involved replacing at least one layer with graphene [12, 16], or a graphene derivative [1], or other carbon structures, ie single-walled nanotubes [1, 17], so this exciting prospect will be the focus of our discussion on future directions.

VI.1. Graphene electrodes

As mentioned, there has been much work in trying to replace ITO as the transparent electrode, given its lessened transparency in the infrared, the scarcity (and thus expense) of indium, and its brittle nature (which voids some of the advantages of flexible OPVs). Graphene, on other hand, is weakly absorbing and mechanically strong and flexible, though unfortunately less conductive.

The heightened resistivity and poor interfacial properties of graphene tended to limit cell efficiencies to the order of 1% [12], but several approaches have been demonstrated to improve the effectiveness of graphene as a transparent electrode, including stacked layers with chemical doping and hybrid structures with metal grids.

Doping multilayer graphene with HNO_3 or $SOCl_2$ has been shown to reduce its sheet resistance by a factor of two (from 850Ω/sq to 450Ω/sq [11], or from 274Ω/sq to 119Ω/sq [10]), with nearly unchanged transmittances in visible spectrum, and such devices have so far acheived efficiencies of 2.6% [11] - 2.86% [10].

Another approach [16] to improving the efficiency of these layers focuses on the effectiveness of the graphene interface with the hole-transport layer. Because graphene is hydrophobic, researchers have experienced difficulties acheiving uniform coatings of aqueous solution-processed PEDOT:PSS on graphene, and the poor interface decreases the desired diode-like rectification properties of the hole-transport layer. And the doping techniques which improve the hydrophillicity of graphene also tend to worsen its conductivity. On the other hand, a thin layer of PEDOT:PEG, which can be applied from organic solvents, coats more readily onto the graphene, and provides a compatible interface for the PEDOT:PSS. These devices have demonstrated efficiences of 2.9%, which places them within 10-15% of the efficiencies of ITO-based devices with the same architecture [16].

Alternatively, the effectiveness of single-layer graphene electrodes has shown improvement under the addition of a metal (Au) grid [12]. Graphene monolayers with 200µm × 200µm Au grids have demonstrated sheet resistances of 22Ω/sq and transmittances of 81.4% (at 550nm), comparable to ITO/glass electrodes (16Ω/sq, 82.8% transmittance). Such devices have reached effiencies of 3.1%.

VI.2. Active layers

Not only are carbon-materials appearing as electrodes, but single-walled carbon nanotubes (SWCNTs) have been demonstrated seperately as both donors and acceptors [1].

Acting as acceptors in combination with polymer donors (P3HT), the SWCNTs have so far demonstrated efficienies up to .72%, and in these applications, precise control over the structure and morphology of the active layer has been vital [17]. For instance, the electronic properties of the nanotubes are strongly dependent on their diameter, d: large diameters lead to lower exciton binding energies (which scale as $\sim 1/d^{11}$), and better carrier mobility ($\sim d^2$), whereas smaller diameters provide greater band offsets and more efficient exciton dissociation. (The optimal diameter for this purpose seems to be somewhere in the range of 1.3-1.5nm.) Excitingly, the P3HT:SWCNT morphology appears to be a vivid realization of the ideal bulk heterojunction, as discussed in Figure 15.

Alternatively, acting as donors in combination with PCBM acceptors, SWCNT-based, polymer-free cells have reported efficiencies as high as 1.3% [1]. Although this is, so far, lower than efficiencies found in polymer-based cells, the theoretical limits for this structure are near 13%, as compared with the theoretical limits for polymer-based cell of about 11% (which have been nearly attained in laboratory settings). These structures also demonstrate much greater photostability than their polymer counterparts. Optimization of the nanotube diameter is again important, but the best structures of this

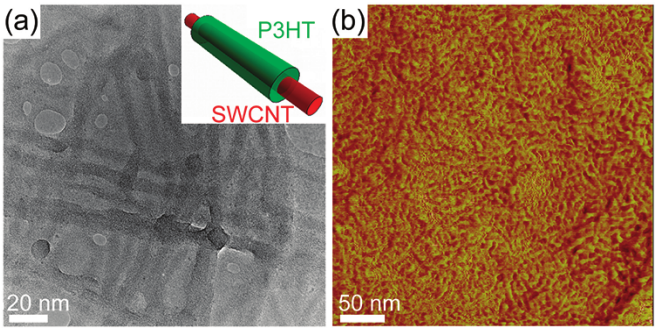

FIG. 15: The "worm-like" morphology in the above TEM (a) and AFM (b) images of P3HT:SWCNT BHJs show nanofilaments of diameters around 10nm, which is about ten times larger than the SWCNTs themselves. The schematic in (a) shows that this results from P3HT wrapping around each SWCNT, thus realizing a maximal D-A interface area. Reprinted from [17].

type have actually incorporated a third carbon-material, reduced graphene oxide (rGO), to improve the bandgap structure, as explained in Figure 16.

In any of the above forms, or more (eg interconnects, and buffer or interfacial layers [1]), the prospect of putting science's latest carbon supermaterials to work in OPV design is an exciting approach.

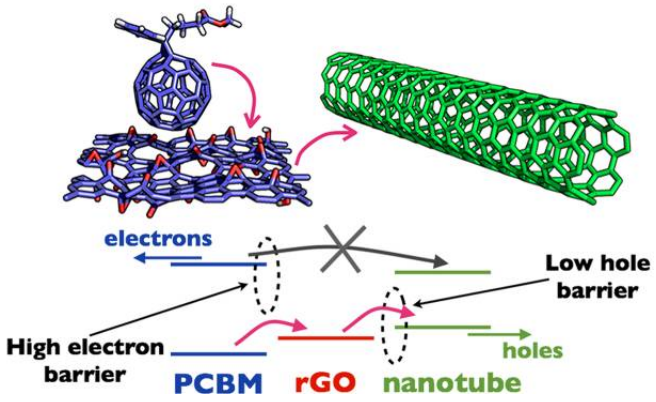

FIG. 16: Band structure for PCBM:rGO:SWCNT active layers. The reduced graphene oxide layer aligns well with the HOMO levels of the PCBM and the nanotube, but creates a large Schottky-type barrier to oppose electron transfer. This asymmetry creates an excellent one-way path for the dissociation of excitons photogenerated in the PCBM. Reprinted from [1].

VII. CONCLUSION AND OUTLOOK

Clearly, bulk heterojunction organic photovoltaics is still a rapidly emerging technology which, by means of a great variety of techniques representing input from many different fields, comes closer every year to a commercially

viable solar power solution. Some reports suggest [7] or argue [18] that OPVs will supply a significant portion of the world's power in the coming decades, whereas less optimistic market analyses [13] claim that OPVs will not beat inorganics in sheer cost, but still find important applications for the flexibility and versatility of the devices. There are still many challenges to overcome, but it is clear that interdisciplinary materials engineering will be at the forefront of bringing this device to the market.

[1] Bernardi, Lohrman, Kumar, Kirkeminde, Ferralis, Grossman, and Ren. "Nanocarbon-based Photovoltaics." *ACS Nano* 6 (2012) 8896-8903.

[2] Cheng, Yang, and Hsu. "Synthesis of Conjugated Polymers for Organic Solar Cell Applications." *Chem. Rev.* 109 (2009), 5868-5923.

[3] Cheyns, Poortmans, and Heremans. "Analytical model for the open-circuit voltage and its associated resistance in organic planar heterojunction solar cells." *Phys. Rev. B* 77 (2008), 165332.

[4] Corkish, Chan, and Green. "Excitons in silicon diodes and solar cells: A three-particle theory." *Amer. Inst. Phys* 79 (1996), 195-203.

[5] Coropceanu et al. "Charge Transport in Organic Semiconductors." *Chem. Rev 107* (2007), 926-952.

[6] Deibel, Carsten and Dyakonov, Vladimir. "Polymer-fullerene bulk heterojunction solar cells." *Rep. Prog. Phys.* 27 (2010), 096401.

[7] Ginley, Green, and Collins. "Solar Energy Conversion Toward 1 Terawatt." *MRS Bull.* 33 (2008), 355364.

[8] Howe, Roger T. and Sodini, Charles G. *Microelectronis: an Integrated Approach.* Prentice Hall Electronics, 1997.

[9] Hull, Robert. *Properties of Crystalline Silicon.* (INSPEC, 1999).

[10] Jung, Na, Kim, and Kang. "Organic photovoltaic devices with low resistance multilayer graphene transparent electrodes." *J. Vac. Sci. Technol. A* 30 (2012), 050604.

[11] Lee, Yeo, Ji, Cho, Kim, Na, Lee, and Lee. "Flexible organic solar cells composed of P3HT:PCBM using chemically doped graphene electrodes." *Nanotechnology* 23 (2012) 344013.

[12] Lin, Choy, Zhang, Xie, Xin, and Leung. "Semi-transparent organic solar cells with hybrid monolayer graphene/metal grid as top electrodes." *Appl. Phys. Lett.* 102 (2013), 113303.

[13] "Organic PV Market Prospects Down." *Solar Novus Today.* [Publicly available report regarding private market analysis.]

[14] Søndergaard, Helgesen, Jørgensen, and Krebs. "Fabrication of Polymer Solar Cells Using Aqueous Processing for All Layers Including the Metal Back Electrode." *Adv. Energy. Mater.* (2011) 1, 68.

[15] Søndlsasdrgaard, Hösel, Angmo, Larsen-Olsen, and Krebs. "Roll-to-roll fabrication of polymer solar cells." textitMaterials Today 15 (2012), 36-49.

[16] Park et al. "Interface engineering of graphene for universal applications as both anode and cathode in organic photovoltaics." *Sci. Rep.* 3 (2013), 1581.

[17] Ren, Bernardi, Lunt, Bulovic, Grossman, Gradeĉak. "Toward Efficient Carbon Nanotube/P3HT Solar Cells: Active Layer Morphology, Electrical, and Optical Properties." *Nano Letters.* dx.doi.org/10.1021/nl202796u

[18] Su, Lan, and Wei. "Organic photovoltaics." *Materials Today* 15 (2012), 554-562.

[19] Yu, Gao, Hummelen, Wudl, and Heeger. "Polymer Photovoltaic Cells: Enhanced efficiencies via a Network of Internal Donor-Acceptor Heterojunctions." *Science* 270 (1995), 1789-1791.